

Structural and magnetic properties of $\text{YFe}_{1-x}\text{Co}_x\text{O}_3$ ($0.1 \leq x \leq 0.5$) perovskite nanomaterials synthesized by co-precipitation method

Nguyen Anh Tien¹, Chau Hong Diem¹, Nguyen Thi Truc Linh¹, V. O. Mittova², Do Tra Huong³, I. Ya. Mittova⁴

¹Ho Chi Minh City University of Education, Ho Chi Minh City, Vietnam

²Burdenko Voronezh State Medical University, Voronezh, 394036, Russia

³Thai Nguyen University of Education, Thai Nguyen University, Vietnam

⁴Voronezh State University, Voronezh, 394018, Russia

anhvienhcmup@gmail.com, hongdiem.chau@gmail.com, linhttn2811@gmail.com, vmittova@mail.ru, dotrahuong@gmail.com, imittova@mail.ru

PACS 75.50.Cc, 81.07.Wx

DOI 10.17586/2220-8054-2018-9-3-424-429

$\text{YFe}_{1-x}\text{Co}_x\text{O}_3$ ($0.1 \leq x \leq 0.5$) perovskite-type nanomaterials were successfully synthesized by the chemical co-precipitation method via the hydrolysis of Y(III), Fe(III) and Co(II) cations in boiling water using 5 % aqueous KOH solution as a precipitating agent. Along with the increase of cobalt ion concentration (x values, from 0.1 to 0.5), there was an decrease in the crystallite size nanomaterials (from 25.68 to 22.89 nm), as well as in the lattice constants ($a = 5.5781 - 5.5217 \text{ \AA}$; $b = 5.2732 - 5.2177 \text{ \AA}$, $c = 7.5902 - 7.5009 \text{ \AA}$; $V = 223.26 - 216.11 \text{ \AA}^3$), but there was an increase in the magnetic parameters including coercive force ($H_c = 88.86 \text{ Oe}$), remnant magnetization ($M_r = 0.031 - 0.268 \text{ emu/g}$), saturation magnetization ($M_s = 0.413 - 1.006 \text{ emu/g}$) and maximum energy product ($(\text{BH})_{\text{max}} = 0.413 - 1.006 \text{ emu/g}$).

Keywords: nanomaterial, co-doped YFeO_3 , perovskite, co-precipitation.

Received: 15 March 2018

Revised: 27 March 2018

1. Introduction

In general, ABO_3 perovskite-type materials are dielectric antiferromagnetic, which can be changed to ferromagnetic by doping it with impurity ions [1–4], especially, in the case of the perovskite-type materials that have rare-earth elements (R) at A sites and Fe(III) ions at the B sites. The reason is the magnetic moment of iron in RFeO_3 is shifted slightly. When transition metals, which have the changed ionic radius at the variable oxidation states, are doped in the structure of RFeO_3 , it may cause an exchange interaction and indirectly lead to ferromagnetic properties. As a ferromagnetic material, perovskites can have interesting properties such as thermoelectric effect, giant magneto-caloric effect (GMCE), giant magneto-resistance (GMR) or spin glass state at low temperature. Thus, perovskite-type materials, particularly at the nano scale, can be applied in the fields of catalysts, solid-oxide fuel cells (SOFCs), chemical sensors, semiconductors, etc. [5–7]. Recently, Co-doped YFeO_3 materials have attracted extensively studying thanks to their interesting magnetic properties that may be changed because of the variable oxidation and spin states of cobalt, as well as its concentration in the solid solution [8].

There are numerous methods to synthesize RFeO_3 nanomaterials such as sol-gel combustion, sol-gel citrate or thermal hydrolysis, etc. [2–4, 9–11]. However, the preparation of the nanomaterials having RFeO_3 single phase by the mentioned methods requires the investigation of many factors including heating temperature and retention time, pH, stoichiometric ratio between the components, etc. As a result, the optimal conditions were difficult to be determined, and the formation of impurity phases such as Fe_3O_4 , YFe_2O_4 or $\text{Y}_3\text{Fe}_5\text{O}_{12}$ [12, 13] might have a negative impact on the quality of the obtained materials. In our previous research [14–16], the perovskite nanomaterials were successfully synthesized by co-precipitation method via the hydrolysis of transition metal ions in boiling water. This paper presents the results of the structural and magnetic properties of Co-doped YFeO_3 nanomaterials prepared by co-precipitation method via the hydrolysis of Y(III), Fe(III) and Co(II) cations in boiling water using 5 % aqueous KOH solution as a precipitating agent.

2. Materials and methods

2.1. Materials

In this research, $\text{Y}(\text{NO}_3)_3 \cdot 6\text{H}_2\text{O}$ (Merck, > 99 %), $\text{Fe}(\text{NO}_3)_3 \cdot 9\text{H}_2\text{O}$ (Merck, ≥ 99 %), $\text{Co}(\text{NO}_3)_2 \cdot 6\text{H}_2\text{O}$ (Merck, ≥ 99 %), KOH (Merck, 99 %) were used for the synthesis of $\text{YFe}_{1-x}\text{Co}_x\text{O}_3$ ($0.1 \leq x \leq 0.5$) perovskite-type nanomaterials.

2.2. Methods

Co-doped $YFeO_3$ were prepared via the process shown in Fig. 1. A mixture of $Y(NO_3)_3 \cdot 6H_2O$, $Fe(NO_3)_3 \cdot 9H_2O$ and $Co(NO_3)_2 \cdot 6H_2O$ salts with the stoichiometric ratio of Y(III) : Fe(III) : Co(II) = 1 : (1 - x) : x ($x = 0.1; 0.15; 0.2; 0.25; 0.3$ and 0.5) was dissolved in distilled water. This solution was added to a glass vessel containing hot water ($t^\circ > 90^\circ C$) and stirred continuously. And then, the obtained mixture was cooled down to the room temperature ($25 - 30^\circ C$), slowly added an excess KOH 5 % solution until the pH greater than 7. The mixture was stirred continuously for 30 mins, and settled for 15 mins. The precipitate was separated from the solution by filtration, washed with distilled water, left to dry at the room temperature and ground into powder.

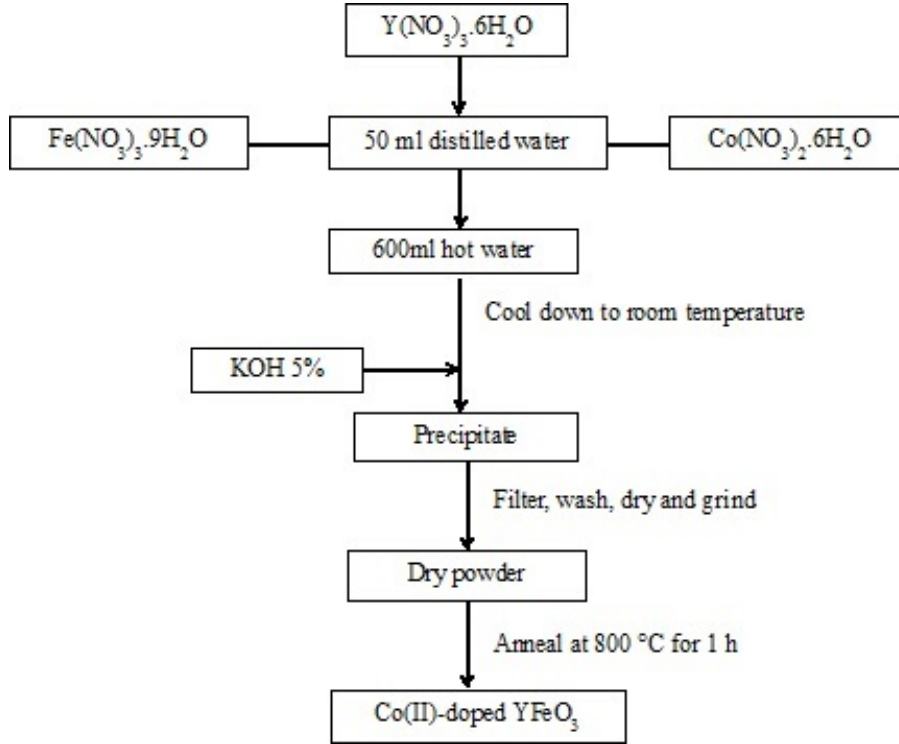


FIG. 1. Flow chart for synthesis of Co-doped $YFeO_3$ by co-precipitation method

All precipitates were converted to perovskite-type materials by annealing at $800^\circ C$ for 1 hour with a heating rate of 10 K/min. The annealing condition was determined according to the previous results [14, 17].

Phase composition of the synthesized samples was identified by powder X-ray diffraction (XRD) with a D8-ADVANCE diffractometer (Germany) using $CuK\alpha$ radiation ($\lambda = 0.154056$ nm), $2\theta = 20 - 80^\circ$, a scan rate of $0.02^\circ s^{-1}$. Average size (nm) of crystal phase was calculated by Debye-Scherrer formula:

$$D_{XRD} = \frac{k\lambda}{\beta \cos \theta}, \quad (1)$$

where k is the shape factor (for the orthorhombic structure, $k = 0.9$); λ is the X-ray wavelength (nm); β is the full width at half maximum (rad) and θ is the position of the diffraction peak.

Lattice constants a , b , c and the unit cell volume V were determined thanks to the X'pert High Score Plus 2.2b software.

Particle size and morphology of $YFe_{1-x}Co_xO_3$ nanomaterials were determined by transmission electron microscopy (TEM) with a JEOL-1400 microscope (Japan). Elemental composition of the samples was determined by energy-dispersive X-ray spectroscopy (EDX) with a FESEM S-4800 spectrometer (Japan). Magnetic parameters of the samples (coercive force H_c , remnant magnetization M_r , saturation magnetization M_s) were carried out at room temperature by a vibrating sample magnetometer (VSM) MICROSENE EV11 (Japan).

3. Results and discussion

3.1. Crystal structure

Figure 2 presented the XRD patterns of $\text{YFe}_{0.8}\text{Co}_{0.2}\text{O}_3$ nanomaterial and component oxides which were prepared via the process shown in Fig. 1 (after annealing at $800\text{ }^\circ\text{C}$ for 1 hour). The results showed that $\text{YFe}_{0.8}\text{Co}_{0.2}\text{O}_3$ nanomaterial was pure perovskite-type, particularly, the peaks of YFeO_3 and Co-doped YFeO_3 were coincident with those of YFeO_3 orthoferrite phase (Card no. 00-039-1489 [18]). The diffraction peaks of oxide impurities cannot be identified in the XRD results. Noticeably, Co_3O_4 oxide was obtained instead of CoO because $\text{Co}(\text{OH})_2$ hydroxide can be oxidized and decomposed after annealing at high temperature [19]:

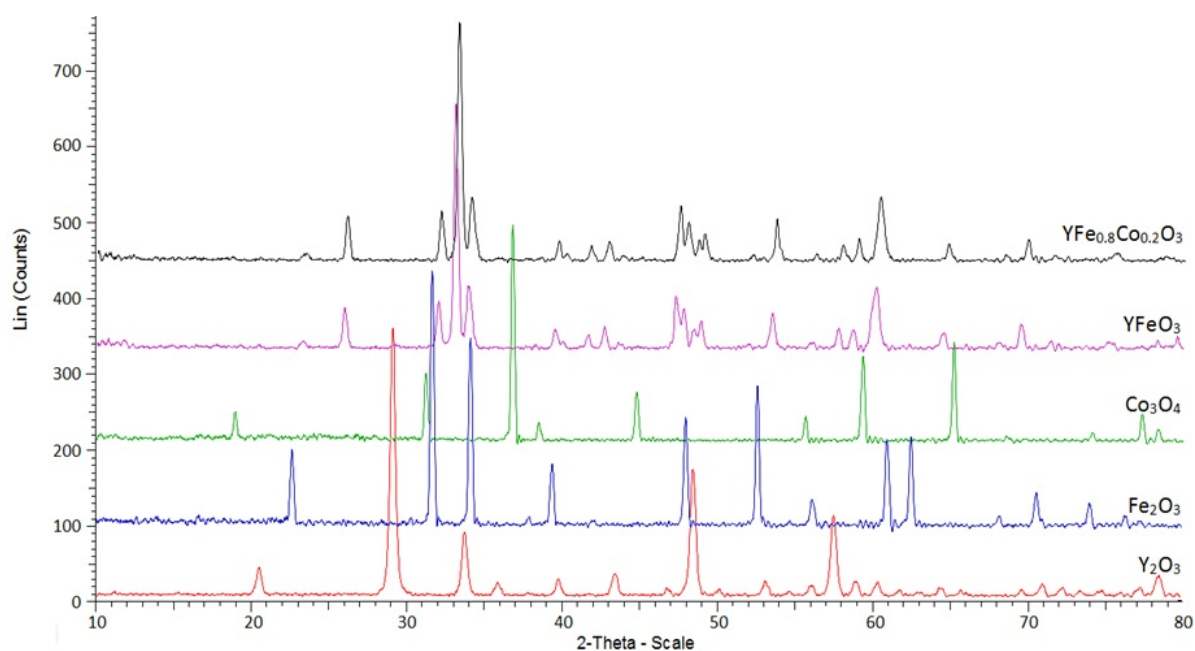
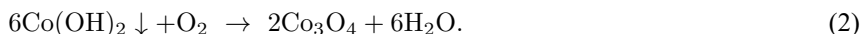


FIG. 2. XRD patterns of $\text{YFe}_{0.8}\text{Co}_{0.2}\text{O}_3$, YFeO_3 and Y_2O_3 , Fe_2O_3 , Co_3O_4 oxides annealed at $800\text{ }^\circ\text{C}$ for 1 hour

This result indicated that Co ions existed in both (II) and (III) oxidation states in the crystal lattice of YFeO_3 .

The XRD patterns of $\text{YFe}_{1-x}\text{Co}_x\text{O}_3$ ($0.1 \leq x \leq 0.5$) samples (Fig. 3) showed the structures of the samples were single-phase perovskites, particularly, they were in the orthorhombic structure with space group $Pnma$, No. 62. This proved that Fe(III) was partly substituted by Co(II)/Co(III). When the concentration of Co ions increased, XRD peaks shifted toward a higher 2θ (right shift) and gradually broadened while the intensity of peaks decreased. Consequently, there was a decrease of lattice parameters and crystal size (Fig. 4A and Table 1). The similar results were published in the previous researches [1, 16, 17].

The results shown in Table 1 showed that lattice parameters of $\text{YFe}_{1-x}\text{Co}_x\text{O}_{3\pm\delta}$ samples decreased in parallel of the increase of the dopant concentration. The substitution of Fe^{3+} ions ($r_{\text{Fe}^{3+}} = 0.65\text{ \AA}$ [19]) by smaller Co^{3+} ions ($r_{\text{Co}^{3+}} = 0.55\text{ \AA}$ [19]) led to the reduction of unit cell parameters following to Vegard's law for ideal solid solution.

Crystal sizes of $\text{YFe}_{1-x}\text{Co}_x\text{O}_{3\pm\delta}$ samples calculated by Debye-Scherrer formula (1) were in the range of 22 to 26 nm. The decrease in the values of crystal size in parallel of the increase of Co concentration can be explained by the substitution of Fe^{3+} ions by Co^{3+} ions, which led to the lattice distortion, the higher internal stress and the limitation of growing of crystalline.

3.2. Elemental composition

EDX spectra showed that the compositions of $\text{YFe}_{1-x}\text{Co}_x\text{O}_3$ samples included Y, Fe, Co and O, without impurity element. The empirical formulas obtained from the elemental analysis were in excellent agreement with the suggested formulas (Table 2).

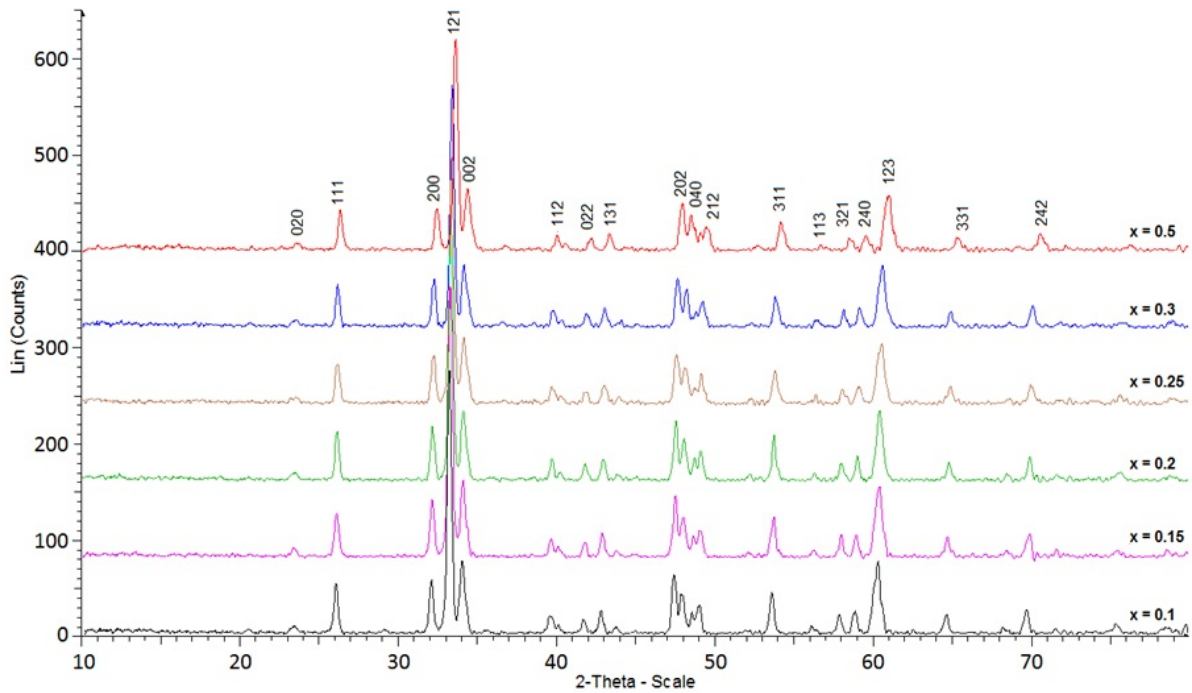


FIG. 3. XRD patterns of $YFe_{1-x}Co_xO_3$ samples annealed at $800\text{ }^\circ\text{C}$ for 1 hour

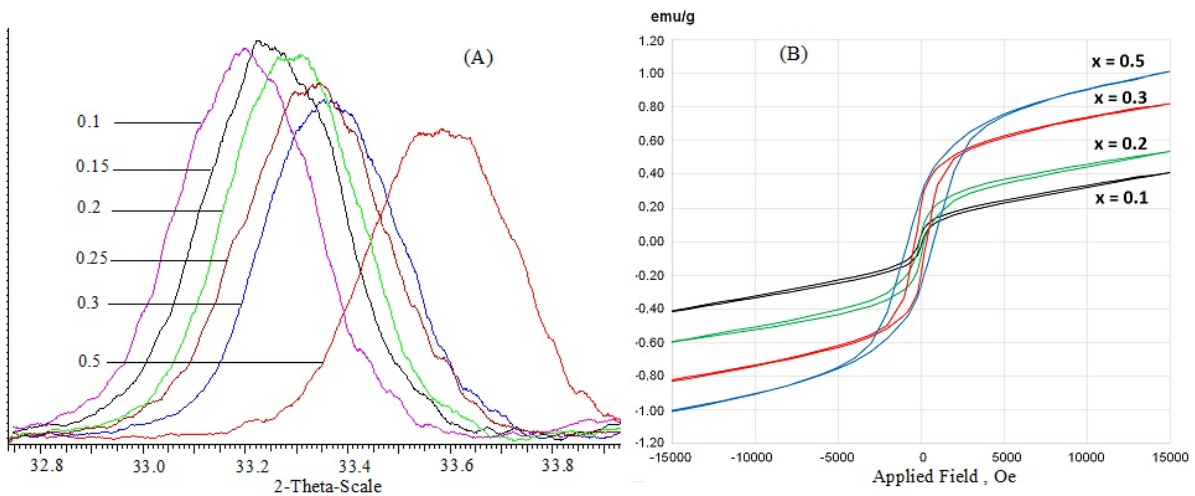


FIG. 4. Slow-scan XRD patterns of peak (121) (A) and field dependence of the magnetization (B) of $YFe_{1-x}Co_xO_3$ nanomaterials annealed at $800\text{ }^\circ\text{C}$ for 1 h

3.3. Morphology

TEM images of $YFe_{1-x}Co_xO_3$ samples ($x = 0.1$; 0.3 and 0.5) (Fig. 5) showed that the shape and size of nanoparticles synthesized were quite homogeneous. Particularly, the particles were in spherical or slightly angular shapes, with an average size of $30 - 50\text{ nm}$.

3.4. Magnetic properties

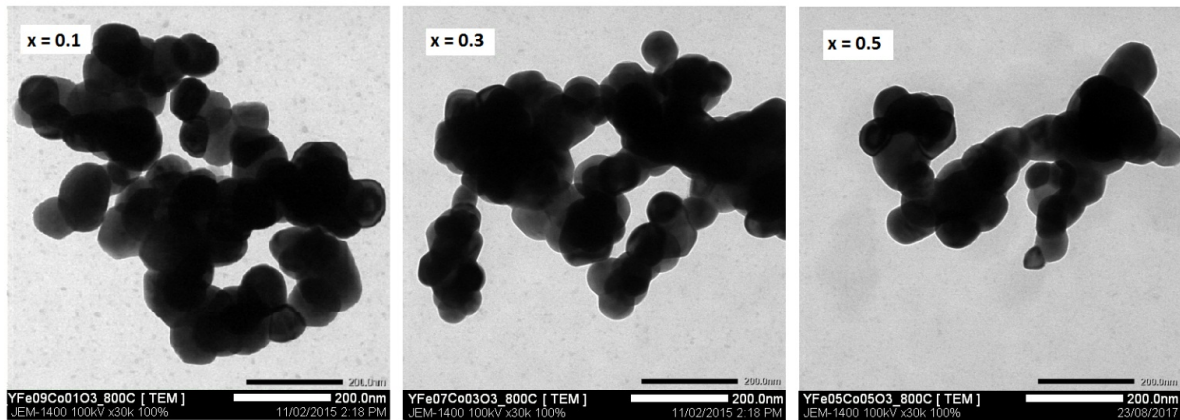
The magnetic parameters of the samples proved that Co substitution impacted not only on the structure but also on magnetic properties of the nanoparticles synthesized (Fig. 5B and Table 2). When the amount of Co ions in $YFeO_3$ crystal lattice increased, the magnetic parameters including H_c , M_r and M_s increased, and were significantly higher than those of the original $YFeO_3$ material [14, 17]. This can be explained by the increase of magnetocrystalline anisotropy because the substitution of Co into the sites of Fe. Besides, Co substitution also

TABLE 1. Lattice parameters and the values of crystal size of $\text{YFe}_{1-x}\text{Co}_x\text{O}_3 \pm \delta$ nanomaterials

$\text{YFe}_{1-x}\text{Co}_x\text{O}_3$	2θ (121), °	D_{XRD} , nm	a , Å	b , Å	c , Å	V , Å ³
$x = 0.1$	33.1913	25.68	5.5781	5.2732	7.5902	223.26
$x = 0.15$	33.2616	25.67	5.5694	5.2625	7.5758	222.04
$x = 0.2$	33.2792	24.44	5.5648	5.2619	7.5708	221.68
$x = 0.25$	33.3330	24.18	5.5575	5.2580	7.5551	220.77
$x = 0.3$	33.3668	23.96	5.5524	5.2505	7.5482	220.05
$x = 0.5$	33.5797	22.89	5.5217	5.2177	7.5009	216.11

TABLE 2. EDX results and magnetic properties of $\text{YFe}_{1-x}\text{Co}_x\text{O}_3$ materials

$\text{YFe}_{1-x}\text{Co}_x\text{O}_3$	Nominal composition	Actual composition	H_c , Oe	M_r , emu/g	M_s , emu/g	$(\text{BH})_{\text{max}}$, emu/g
$x = 0$	YFeO_3 [15]	$\text{YFe}_{1.02}\text{O}_{3.32}$	53.36	0.019	0.390	0.390
$x = 0.1$	$\text{YFe}_{0.9}\text{Co}_{0.1}\text{O}_3$	$\text{YFe}_{0.88}\text{Co}_{0.11}\text{O}_{3.37}$	88.86	0.031	0.413	0.413
$x = 0.2$	$\text{YFe}_{0.8}\text{Co}_{0.2}\text{O}_3$	$\text{YFe}_{0.79}\text{Co}_{0.21}\text{O}_{3.28}$	132.66	0.075	0.569	0.569
$x = 0.3$	$\text{YFe}_{0.7}\text{Co}_{0.3}\text{O}_3$	$\text{YFe}_{0.69}\text{Co}_{0.28}\text{O}_{3.67}$	352.16	0.207	0.825	0.825
$x = 0.5$	$\text{YFe}_{0.5}\text{Co}_{0.5}\text{O}_3$	$\text{YFe}_{0.51}\text{Co}_{0.51}\text{O}_{3.43}$	781.46	0.268	1.006	1.006

FIG. 5. TEM images of $\text{YFe}_{1-x}\text{Co}_x\text{O}_3$ nanomaterials annealed at 800 °C for 1 h

led to a change in Fe–O–Fe angles, as well as an oxidation of a small amount of Fe^{3+} ions to Fe^{4+} ions to compensate the charge caused by the appearance of Co^{2+} at the sites of Fe^{3+} . Similar results were mentioned by other authors [16, 17, 20].

Noticeably, with $x \geq 0.2$, YFeO_3 changed gradually from a soft magnetic material ($H_c < 100$ Oe) to a hard magnetic material with high coercive force ($H_c \gg 100$ Oe, especially with $x = 0.5$). This proved that magnetic properties of YFeO_3 material can be changed by doping Co, thus the applicability of this material can be extended in many devices requiring the soft magnetic material (cores of transformers, electromagnets, magnetic conductors) and also the ones requiring the hard magnetic material (permanent magnets or recorders).

4. Conclusions

$\text{YFe}_{1-x}\text{Co}_x\text{O}_3$ ($0.1 \leq x \leq 0.5$) perovskite-type nanomaterials were successfully prepared by the chemical coprecipitation method via the hydrolysis of cations in hot water ($t^\circ \geq 90$ °C) with KOH 5 % as a precipitating agent. Along with the increase of Co doping, the values of crystal size and unit cell volume decreased from 26 nm to 22

nm, from 224 \AA^3 to 216 \AA^3 , respectively, while those of the coercive force (H_c), remnant magnetization (M_r), saturation magnetization (M_s) and maximum energy product (BH_{max}) increased from 88.86 to 781.46 Oe, from 0.031 to 0.268 emu/g, from 0.413 to 1.006 emu/g and from 0.413 to 1.006 emu/g, respectively. The substitution of Co into the sites of Fe led to a change of the crystal lattice, which affected the magnetic properties of $YFeO_3$ perovskite-type nanomaterials.

References

- [1] Nishiyama Sh., Asako I., Iwadate Ya., Hattori T. Preparation of $Y(Mn_{1-x}Fe_x)O_3$ and Electrical Properties of the Sintered Bodies. *Open Journal of Inorganic Chemistry*, 2015, **5**, P. 7–11.
- [2] Gimaztdinova M.M., Tugova E.A., Tomkovich M.V., Popkov V.I. Synthesis of $GdFeO_3$ nanocrystals. *Condensed Matter and Interfaces*, 2016, **18** (3), P. 422–431.
- [3] Bachina A., Ivanov V.A., Popkov V.I. Peculiarities of $LaFeO_3$ nanocrystals formation via glycine-nitrate combustion. *Nanosystems: Physics, Chemistry, Mathematics*, 2017, **8** (5), P. 647–653.
- [4] Martinson K.D., Kondrashkova I.S., Popkov V.I. Synthesis of $EuFeO_3$ nanocrystals by glycine-nitrate combustion method. *Russian Journal of Applied Chemistry*, 2017, **90** (8), P. 980–985.
- [5] Lee J., Kim S., Tak Y., Yoon Y.S. Study on the LLT solid electrolyte thin film with LiPON interlayer intervening between LLT and electrodes. *Journal of Power Sources*, 2006, **163**, P. 173–179.
- [6] Oemar U., Ang P.S., Hidajat K., Kawi S. Promotional effect of Fe on perovskite $LaNi_xFe_{1-x}O_3$ catalyst for hydrogen production via steam reforming of toluence. *International Journal of Hydrogen Energy*, 2013, **38**, P. 5525–5534.
- [7] Jeffrey W.F. Perovskite oxides for semiconductor-based gas sensors. *Sensors and Actuators B: Chemical*, 2007, **123**, P. 1169–1179.
- [8] Karpinsky D.V., Troyanchuk I.O., et al. Crystal structure and magnetic properties of the $LaCo_{0.5}Fe_{0.5}O_3$ perovskite. *Crystallography Report*, 2006, **51** (4), P. 596–600.
- [9] Maiti R., Basu S., Chakravorty D. Synthesis of nanocrystalline $YFeO_3$ and its magnetic properties. *Journal of Magnetism And Magnetic Materials*, 2009, **321**, P. 3274–3277.
- [10] Lomanova N.A., Gusarov V.V. Influence of synthesis temperature on $BiFeO_3$ nanoparticles formation. *Nanosystems: Physics, Chemistry, Mathematics*, 2013, **4** (5), P. 696–705.
- [11] Feng C., Ruan Sh., et al. Ethanol sensing properties of $LaCo_xFe_{1-x}O_3$ nanoparticles: Effects of calcination temperature, Co-doping, and carbon nanotube-treatment. *Sensors and Actuators B*, 2011, **155** (1), P. 232–238.
- [12] Chithralekha P., Murugeswari C., Ramachandran K., Srinivasan R. The study on ultrasonic velocities of $Co_xFe_{3-x}O_4$ nanoferrofluid prepared by co-precipitation method. *Nanosystems: Physics, Chemistry, Mathematics*, 2016, **7** (3), P. 558–560.
- [13] Jacob K.T., Rajitha G. Nonstoichiometry, defects and thermodynamic properties of $YFeO_3$, YFe_2O_4 , $Y_3Fe_5O_{12}$. *Solid State Ionics*, 2012, **224**, P. 32–40.
- [14] Nguyen A.T., Almjasheva O.V., et al. Synthesis and magnetic properties of $YFeO_3$ nanocrystals. *Inorganic Materials*, 2009, **45** (11), P. 1304–1308.
- [15] Nguyen A.T., Mittova I.Ya., et al. Influence of the preparation conditions on the size and morphology of nanocrystalline lanthanum orthoferrite. *Glass Physics and Chemistry*, 2008, **34** (6), P. 756–761.
- [16] Knurova M.V., Mittova I.Ya., et al. Effect of the degree of doping on the size and magnetic properties of nanocrystals $La_{1-x}Zn_xFeO_3$ synthesized by the sol-gel method. *Russian Journal of Inorganic Chemistry*, 2017, **62** (3), P. 281–287.
- [17] Nguyen A.T., Hap M.C. Study on synthesis of modified $Y_{1-x}Cd_xFeO_3$ nanosized material by co-precipitation method. *Vietnam Journal of Chemistry*, 2016, **54** (5e 1, 2), P. 237–241.
- [18] JCPDC PCPDFWIN: A Windows Retrieval/Display program for Accessing the ICDD PDF - 2 Data base, International Centre for Diffraction Data, 1997.
- [19] Housecroft C.E., Sharpe A.G. *Inorganic Chemistry*, 2nd ed. Pearson Prentice Hall, USA, 2005, 949 p.
- [20] Nguyen A.T., Mittova I.Ya., et al. Sol-gel formation and properties of nanocrystals of solid solution $Y_{1-x}Ca_xFeO_3$. *Russian Journal of Inorganic Chemistry*, 2014, **59** (2), P. 40–45.